

3D versus 2D contrast-enhanced sonography in the evaluation of therapeutic response of hepatocellular carcinoma after locoregional therapies: preliminary findings

Tommaso Vincenzo Bartolotta · Adele Taibbi ·
Domenica Matranga · Massimo Midiri ·
Roberto Lagalla

Received: 18 October 2014 / Accepted: 28 January 2015 / Published online: 20 February 2015
© Italian Society of Medical Radiology 2015

Abstract

Objective To investigate diagnostic performance of 3D contrast-enhanced ultrasound (CEUS) compared with 2D CEUS in the assessment of therapeutic response of hepatocellular carcinoma (HCC) treated with locoregional therapies (LRT).

Materials and methods Twenty-three consecutive patients (13 men and 10 women; mean age 65.5 years) with 23 HCCs (size range 1.2–7.2 cm; mean size 2.9 ± 1.4 cm) treated by means of radiofrequency ablation (RFA $n = 9$), transarterial chemoembolization (TACE $n = 8$), combined RFA and TACE ($n = 3$), percutaneous alcoholization ($n = 2$), and wedge resection ($n = 1$) underwent 2D and 3D CEUS 1 month (30 ± 2 days) after treatment. Magnetic resonance ($n = 17$) and computed tomography ($n = 6$) acted as standard of reference (SOR). Two radiologists assessed the absence (complete response CR) or presence (residual tumor RT) of any nodular arterially enhancing area within or along the margin of the treated HCC.

Results Both 2D and 3D CEUS observed CR in 10/23 (43.5 %) HCCs and RT in 11/23 (47.8 %) HCCs. In 1/23 (4.3 %) HCC, RT was documented by SOR and 2D CEUS, but it was not appreciable at 3D CEUS. In 1/23 (4.3 %) HCC, the presence of peripheral residual tumor was suspected by both 2D and 3D CEUS, but it was not confirmed by SOR. No statistically significant difference between 2D and 3D CEUS in depicting either CR or RT was found ($p > 0.05$). Sensitivity, specificity, positive and negative predictive values, and accuracy of 3D CEUS were 91.7 %

[95 % confidence interval (CI) 0.760–1.073], 90.9 % (95 % CI 0.739–1.079), 91.7, 90.9, and 91.3 %, respectively.

Conclusion 2D and 3D CEUS provided similar diagnostic performance in the assessment of therapeutic response of HCC treated with LRT.

Keywords Liver · Contrast-enhanced 3D ultrasound · Hepatocellular carcinoma · Contrast agent

Introduction

Over the past decade, locoregional therapies (LRT) have emerged as a valid alternative to conventional surgery in patients with hepatocellular carcinoma (HCC) [1, 2]. An accurate assessment of therapeutic response is of crucial importance, considering that a complete tumor ablation significantly increases patient survival, whereas residual unablated tumor calls for additional treatment [3, 4]. Imaging modalities play a pivotal role in this task, although they have been reported to be fairly insensitive in demonstrating residual disease after LRT when compared to histology [5]. Computed tomography (CT), Magnetic resonance imaging (MRI), and contrast-enhanced ultrasound (CEUS) suggest a successful procedure when a previously enhancing, hypervascularized HCC nodule shows lack of contrast enhancement after treatment, whereas still viable tumoral tissue is typically depicted as an arterial-enhancing focus with portal venous washout [6].

More recently, three-dimensional contrast-enhanced US technique (3D CEUS) has been reported to improve the study of tumor vascularity, thus allowing the response evaluation of radiofrequency ablation in the three orthogonal planes [7]. Nevertheless, it has been suggested that the spatial resolution of the current 3D probes may be limited,

T. V. Bartolotta (✉) · A. Taibbi · D. Matranga · M. Midiri · R. Lagalla

Department of Radiology, University of Palermo, Via Del Vespro
127, 90129 Palermo, Italy
e-mail: tv_bartolotta@yahoo.com

and volumetric acquisition of the data may be associated with distortion of the volume as a result of motion when using mechanical probes [8].

Hence, we undertook this study in an attempt to investigate diagnostic performance of 3D CEUS compared with 2D CEUS in the assessment of therapeutic response of HCC treated with LRT. The influence of 3D CEUS on clinical outcome was also evaluated.

Materials and methods

Patient population and imaging techniques

Institutional review board approval was obtained and full written informed consent was obtained for this prospective study. Our study complied with the terms of the Declaration of Helsinki [9].

Twenty-three consecutive patients (13 men and 10 women; age range 45–81 years; mean age 65.5 ± 10 years) with 23 HCCs (size range 1.2–7.2 cm; mean size 2.9 ± 1.4 cm) treated by means of radiofrequency ablation (RFA $n = 9$), transarterial chemoembolization (TACE $n = 8$), combined RFA and TACE treatments ($n = 3$), percutaneous alcoholization (PEI $n = 2$), and wedge resection with bipolar radiofrequency electrosurgical device (HABIB $n = 1$) underwent 2D and 3D CEUS 1 month (30 ± 2 days) after treatment.

2D CEUS

Two experienced radiologists (more than 5 years of CEUS of the liver), who were aware of the patients' clinical histories, performed US scanning by means of an iU22 unit (Philips Ultrasound, Bothell, WA, USA), provided with a C5-1 MHz convex array probe and pulse inversion imaging software. A baseline survey examination, including a color/power Doppler (CD/PD) and spectral analysis, was performed. Once set, the US scan parameters—such as focal zone and time gain compensation—were not changed throughout the study. The US contrast agent used in the present study was sulfur hexafluoride (SonoVue, Bracco, Milan, Italy), which was injected intravenously as a 2.4 mL bolus followed by 10 mL of normal sterile saline flush using a 20- or 22-Gauge peripheral intravenous cannula. A low frame rate (5 Hz) and a very low mechanical index (MI), ranging from 0.05 to 0.08, were used for real time imaging. One focus was positioned below the level of the lesion.

Digital cine-loops were registered during both baseline and post-contrast US in the arterial, hepatic venous, and extended hepatic venous or late phase (i.e., 5–40, 55–90, and until 200–300 s from the beginning of injection, respectively).

3D CEUS

In the same session, with an interval time of at least 15 min to allow for contrast clearance of the previous contrast injection, the same radiologist who performed baseline ultrasound and 2D CEUS, also performed 3D CEUS scanning by means of the same iU22 unit provided with a volumetric mechanical V6-2 MHz probe and pulse inversion imaging software. Harmonic imaging was used and image was optimized for size, tissue contrast, and resolution. Depending on the size and depth of each lesion, an appropriate sweep angle (angle range 40–55 degrees) was selected in order to encompass the entire lesion. SonoVue (Bracco, Milan, Italy) was then injected intravenously as a 4.8 mL bolus followed by 10 mL of normal sterile saline flush. We decided to use a full bolus of 4.8 mL of sulfur hexafluoride in order to compensate for some technical advantages of C5-1 MHz probe over V6-2 MHz probe, such as operating frequency and “PureWave technology crystals”, which provide a better nominal penetration power for the C5-1 MHz probe. In suspended respiration, 3D sweep was started and three volumetric datasets were acquired in the arterial, hepatic venous, and extended hepatic venous or late phase (i.e., 25–40, 60–90, and 200–300 s from the beginning of injection, respectively). A very low MI, ranging from 0.06 to 0.08, was used and each volume acquisition lasted 2–4 s depending on the selected sweep angle, with longer acquisition time for greater angles. Each examination lasted about 5 min after bolus injection.

All images and cine-loops were digitally stored both as raw data in a PC-based workstation connected to the US units via a standard Ethernet link and sent to our PACS (Impax, Agfa-Gevaert, Milan, Italy).

Image analysis

Two abdominal radiologists (more than 10 years of experience) randomly reviewed off-line by consensus 2D and 3D CEUS examinations. The readers were not involved in the scanning and were blinded to the final diagnosis, as well as to the identification, clinical histories, and other imaging findings of the patients. Two consecutive interpretation sessions with a 7-day interval to avoid recall bias were held to complete the review process.

3D volumes were reviewed using a commercially available proprietary software (QLAB, Philips Ultrasound, Bothell, WA, USA) approved for clinical use and capable of volume rendering mode and iSlice mode. This latter mode provides the capability of displaying the dataset in multiple, contiguous, parallel 2D slices, similar to CT and MR, in three orthogonal planes, i.e., plane A, which can be translated from front to back, plane B, which can be translated from right to left, and plane C, which can be

translated from above to bottom. In order to better display the region of interest, radiologists were able to freely rotate and zoom the volume and to set several parameters, such as (1) number of slices: range 4–30; (2) interval slice (distance between the individual slices): range 0.1–176 mm; (3) depth (the position of the slices in the volume): range 0.6–150 mm.

For each lesion, the two readers were asked to report size, depth (starting from the skin surface and ending to the deeper aspect of the lesion) and segment location according to Couinaud classification system. The two readers were also asked to report (1) complete response (CR): the absence of any nodular arterially enhancing portion within or at the margin of treated HCC; (2) residual tumor (RT): any nodular arterially enhancing area within or along the margin of the treated HCC [6, 10]. Residual viable tumor was also categorized as (1) ingrowth pattern, when a hypervascular focus was detected within the edge of a treated nodule and (2) outgrowth pattern, when a hypervascular focus was detected around a necrotic treated nodule and in continuity with its border [11]. The presence of a uniform and thin (4–5 to 7–8-mm thick) peripheral rim of contrast enhancement surrounding the treated zone was regarded as benign reactive hyperemia [6]. The time needed for a complete evaluation of each single 3D volumetric dataset, including defining and zooming the area of interest, choosing the appropriate depth, number, and spacing of slices was also measured.

The influence of both methods on clinical outcome was evaluated on a three-point scale: (1) 2D CEUS imaging changed diagnosis and consequently lesion's management (score 1); 3D CEUS and 2D CEUS studies provided the same diagnosis (score 2); 3D CEUS imaging changed diagnosis and consequently lesion's management (score 3).

Reference standard

The final diagnosis was obtained by magnetic resonance imaging (MRI) with hepatocellular specific Gadolinium-based contrast agent ($n = 17$) and multidetector row computed tomography (MDCT) ($n = 6$). MR and CT scans were performed the same day of 2D and 3D CEUS. Diagnostic criteria for complete treatment at MRI/MDCT were the absence of any enhancing portion within or at the margin of the ablation zone during the hepatic arterial phase, as previously reported [12]. Diagnostic criteria for residual viable tumoral tissue at MRI/MDCT were any nodular arterially enhancing area within or along the margin of the treated HCC [10].

Follow-up by means of both CT and/or MRI, laboratory data, and clinical assessment were also used to confirm the diagnosis obtained one month after treatment.

CT

CT studies were performed by means of a 64-slice MDCT (Brilliance 64; Philips Medical Systems, Eindhoven, the Netherlands). Patients received 1.5 mL/kg total body weight of 400 mgI/mL non-ionic contrast agent (Iomeron 400; Bracco Imaging, Milan, Italy) infused using an automated injector (Medrad, Indianola, IA, USA) at a rate of 4 mL/s through a 18–20 Gauge catheter inserted into an antecubital vein. CT was performed immediately before contrast agent administration and during hepatic arterial, hepatic venous, and delayed phases. To determine the scanning delay for the hepatic arterial phase, the time-to-peak aortic enhancement was assessed using an automatic bolus-tracking technique with automated scan-triggering software (Bolus Pro Ultra, Philips Medical Systems, Eindhoven, the Netherlands). Hepatic arterial phase scanning was started automatically 18 s after the trigger threshold (150 HU) was reached at the level of the suprarenal abdominal aorta. The hepatic venous and delayed phases were acquired, respectively, 40 s after the beginning of arterial phase, and 180 s after injection of contrast.

MR imaging

MRI was performed with a 1.5 T MR unit (Signa Excite HDXT, General Electric Healthcare, Milwaukee, WI, USA) using a phased-array multicoil. The MRI protocol included pre-contrast axial breath-hold and respiratory-triggered T2-weighted FSE sequences with and without fat saturation (TR/TE 4,000/76 ms, Flip angle 150°, section thickness 6 mm), unenhanced (in-phase and out-of-phase) T1-weighted (TR/TE 150/4.2–2.1 ms, Flip angle 80°, section thickness 4 mm) and pre-contrast fat-saturated spoiled 3D gradient-recalled echo (GRE) T1-weighted sequences (TR/TE 4.2/2.0 ms, Flip angle 12°, section thickness 3 mm). A triphasic dynamic contrast-enhanced study was obtained after the administration of a IV bolus of 0.1 mmol/kg of gadobenate dimeglumine (MultiHance, Bracco, Italy) injected into an antecubital vein at a flow rate of 2 mL/s through a 20-Gauge intravenous catheter by means of a power injector (MR Spectris; Medrad, Pittsburgh, PA, USA) and flushed by 20 mL of sterile saline solution. Images were acquired using automated bolus detection technique (Smartprep technique, GE Healthcare) during the arterial (16 s after bolus detection), hepatic venous, and delayed phase (60 and 180 s after bolus injection, respectively). The dynamic study was followed by a hepatocellular-specific phase obtained 2 h after the injection of contrast material, with the same scanning parameters.

Table 1 HCC with complete response at 2D and 3D CEUS confirmed by SOR

Patient/sex/age (years)	Treatment type	Liver segment	HCC size (mm)	Treated lesion depth (mm)
1/M/57	RFA	VII	27	100
2/M/63	RFA	V	16	51
3/M/59	RFA	VI	24	65
4/M/63	TACE	IV	12	39
5/F/72	PEI	VIII	16	82
6/M/79	RFA	V	20	50
7/M/65	HABIB	V	42	35
8/F/81	RFA	V	16	40
9/F/63	TACE	VII	29	120
10/M/59	RFA	VIII	18	69

F female, *M* male, *RFA* radiofrequency ablation, *TACE* transarterial chemoembolization, *PEI* percutaneous alcoholization, *HABIB* resection with bipolar radiofrequency electrosurgical device

Statistical analysis

Statistical analysis was performed by a biostatistician, which was involved in the study design, using a computer software package: StataMP Version 11.0 (StataCorp LP, College Station, TX, USA).

On the basis of SOR findings, detailed lesion-by-lesion analysis was performed, and sensitivity and specificity (diagnostic performance) with 95 % CI for 3D CEUS were calculated. The statistical significance of the difference between 2D CEUS and 3D CEUS in the assessment of therapeutic response of HCC-treated LRT was tested by two-tailed McNemar's test with the continuity correction.

The statistical significance of the difference between complete and incomplete responses for lesions' size and depth was tested through the Kruskal–Wallis equality-of-populations rank test. Statistical significance was considered to be present at a p value of <0.05 .

Results

No adverse events have been registered in our patients during or immediately after the injection of contrast agent.

19/23 (82.6 %) treated HCCs were located in the right lobe, whereas the remaining 4/23 in the left lobe (17.4 %). The lesions were located at a mean depth of 6.5 ± 2.3 cm (depth range 3.5–12 cm).

A complete response, confirmed by SOR, was observed either at 2D and 3D CEUS in 10/23 (43.5 %) HCCs (size range 1.2–4.2 cm; mean size 2.2 ± 0.9 cm) (Table 1; Fig. 1). Seven of these latter patients received RFA ($n = 6$) or HABIB ($n = 1$) procedures and the presence of a thin peripheral rim of benign reactive hyperemia was observed in 2/7 cases (Fig. 2).

In 11/23 (47.8 %) HCCs (size range 2–7.2 cm; mean size 3.7 ± 1.4 cm), a residual tumor was documented by SOR, 2D and 3D CEUS (Table 2; Fig. 3). The RT presented a mean size of 2.9 ± 1.3 cm (size range 1.5–5.2 cm). An

ingrowth pattern was observed in 4/11 (36.4 %) cases, an outgrowth pattern in 5/11 (45.4 %) cases, and a mixed ingrowth/outgrowth pattern in 2/11 (18.2 %) cases.

In 1/23 (4.3 %) case—a 2 cm sized HCC, deeply located (100 mm) in the segment VIII—a residual tumor sized 1.8 cm was documented after RFA by SOR and 2D CEUS, but it was not appreciable at 3D CEUS (Fig. 4).

In the remaining 1/23 (4.3 %) HCC located in segment VI of size 1.5 cm and depth 42 mm, the presence of peripheral residual tumor (10 mm) was suspected after PEI by both 2D and 3D CEUS, but it was not confirmed by SOR (Fig. 5).

The difference between complete and incomplete responses was statistically significant for correlation with lesions' size ($p = 0.006$), but not with lesion's depth ($p = 0.751$).

Overall, in 22/23 [95.6 %, 95 % CI = (87.3–104.0)] cases, 3D CEUS and 2D CEUS studies provided the same diagnosis (score 2), showing excellent intermodality agreement. There was not any statistically significant difference between conventional CEUS and 3D CEUS in depicting either complete response ($p = 1.000$) and residual tumor ($p = 1.000$).

On a lesion-by-lesion basis, sensitivity, specificity, positive and negative predictive values, and accuracy of 3D CEUS were 91.7 % (95 % CI 0.760–1.073), 90.9 % (95 % CI 0.739–1.079), 91.7, 90.9, and 91.3 % respectively.

A complete evaluation of a single 3D volumetric dataset, including defining and zooming the area of interest, choosing the appropriate depth, number, and spacing of slices lasted on average 45.7 ± 21.6 s (range 26–99 s).

Discussion

Since its introduction in clinical settings, three-dimensional ultrasonography (3D-US) has been widely used in gynecology, obstetrics, and cardiology, whereas its use in liver imaging is still limited [13]. Pilot studies have shown that

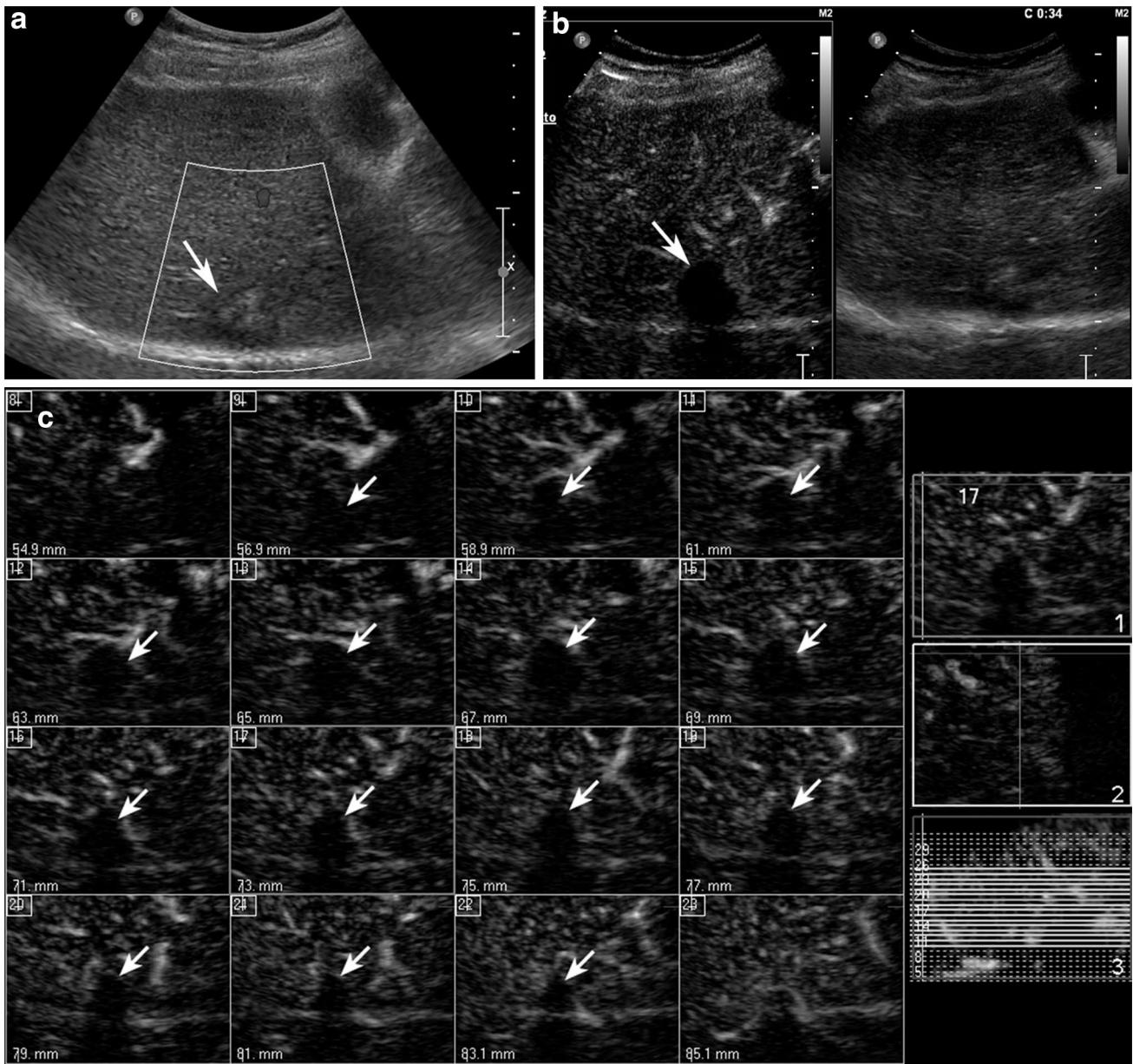


Fig. 1 Complete response after RFTA. **a** Oblique ascending right subcostal baseline US image in a 57-year-old man shows a 2.7-cm-sized inhomogeneous hypo–hyperechoic area in the VII hepatic segment (*arrow*) without detectable flow at color Doppler evaluation

(*box*), **b** at 2D CEUS in the arterial phase (34 s after SonoVue injection), the lesion shows lack of contrast enhancement (*left, arrow*); **c** 3D i-Slice reconstruction (slice thickness 2 mm) confirms the same finding throughout the lesion, slice by slice (*arrows*)

the use of 3D US after the administration of microbubble-based contrast agent (3D CEUS) aids in the characterization of focal liver tumors by evaluating their vascular patterns [14, 15]. Unlike conventional 2D CEUS, 3D CEUS allows the division of structures into tomographic slices in three orthogonal planes, thus providing supplementary information unachievable with 2D CEUS. By presenting several slices continuously, changing thickness and distances between two slices 3D CEUS can make it easier to detect enhancement in different portions of tumors [15]. This

latter feature of 3D CEUS has been suggested to be beneficial in monitoring the response of HCC treated by means of radiofrequency ablation [8, 13]. To our knowledge, this is the first study directly comparing 3D CEUS with 2D CEUS in the assessment of therapeutic response of HCC treated with locoregional therapies. Luo and co-workers have compared 3D CEUS with contrast-enhanced CT in the evaluation of the effect of radiofrequency ablation of HCCs, finding good concordance of 3D CEUS with CT and reporting sensitivity, specificity, and accuracy values for detecting

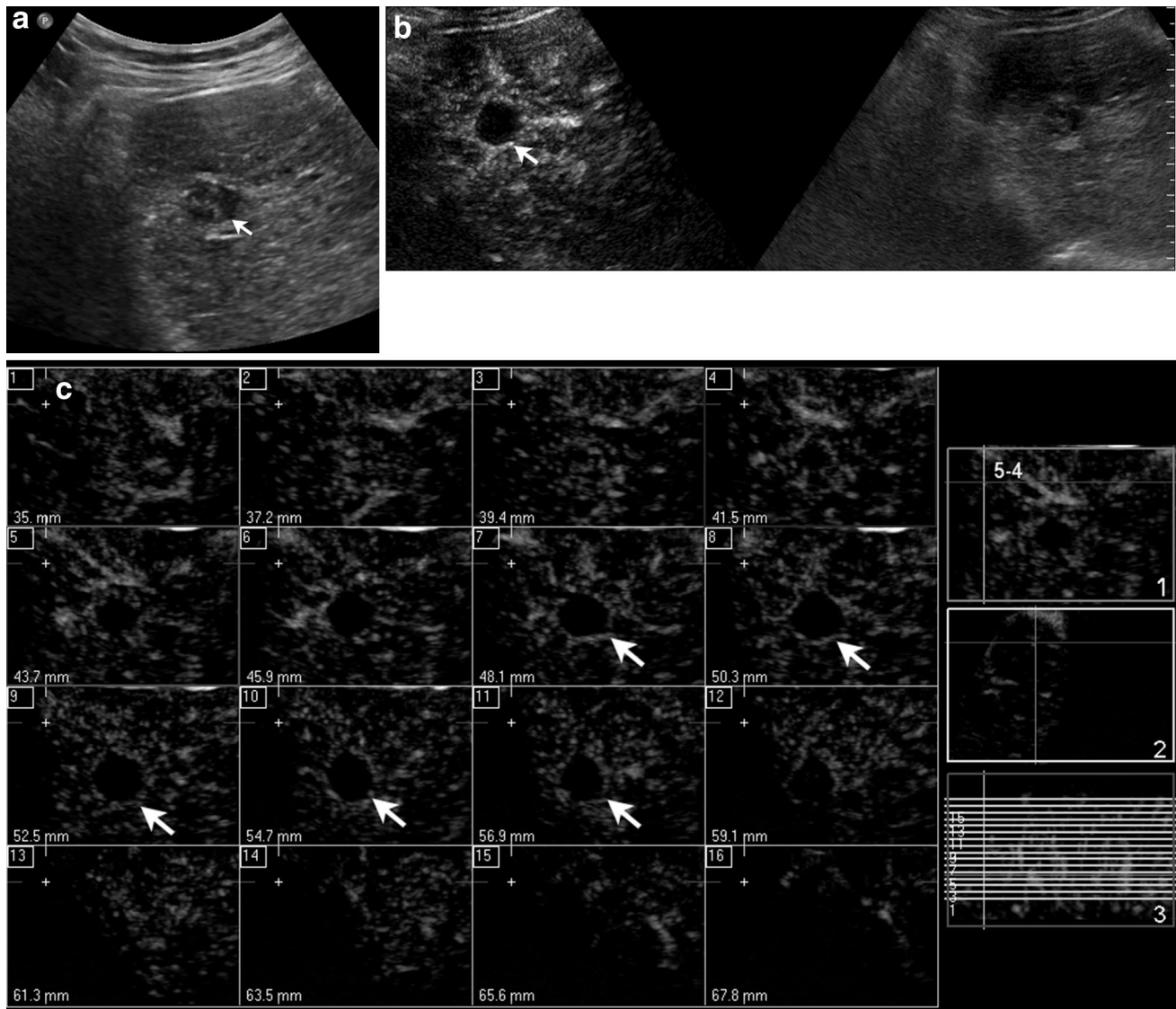


Fig. 2 Rim of hyperemia surrounding a complete RFTA treatment. **a** Oblique ascending right subcostal image in a 63-year-old man reveals an inhomogeneous hypoechoic 1.6-cm-sized area in the V hepatic segment (*arrow*), **b** at 2D CEUS, a thin peripheral rim of contrast

enhancement surrounds the ablated zone in the arterial phase (*left, arrow*); **c** 3D i-Slice reconstruction (slice thickness 2.2 mm) depicts the same finding (*arrows*)

Table 2 HCC with residual tumor at 2D and 3D CEUS confirmed by SOR

Patient/sex/age (years)	Treatment type	Liver segment	HCC size (mm)	Treated lesion depth (mm)
1/F/63	RFA	V	20	40
2/F/79	RFA/TACE	VII	30	49
3/M/71	RFA/TACE	VIII	38	60
4/M/68	TACE	V	25	52
5/M/77	TACE	VIII	40	80
6/F/74	RFA	VI	34	60
7/M/51	TACE	VII	24	54
8/M/61	TACE	III	43	60
9/F/52	TACE	IV	72	75
10/M/69	PEI/TACE	VIII	44	79
11/F/56	TACE	I	33	90

F female, *M* male, *RFA* radiofrequency ablation, *TACE* transarterial chemoembolization, *PEI* percutaneous alcoholization

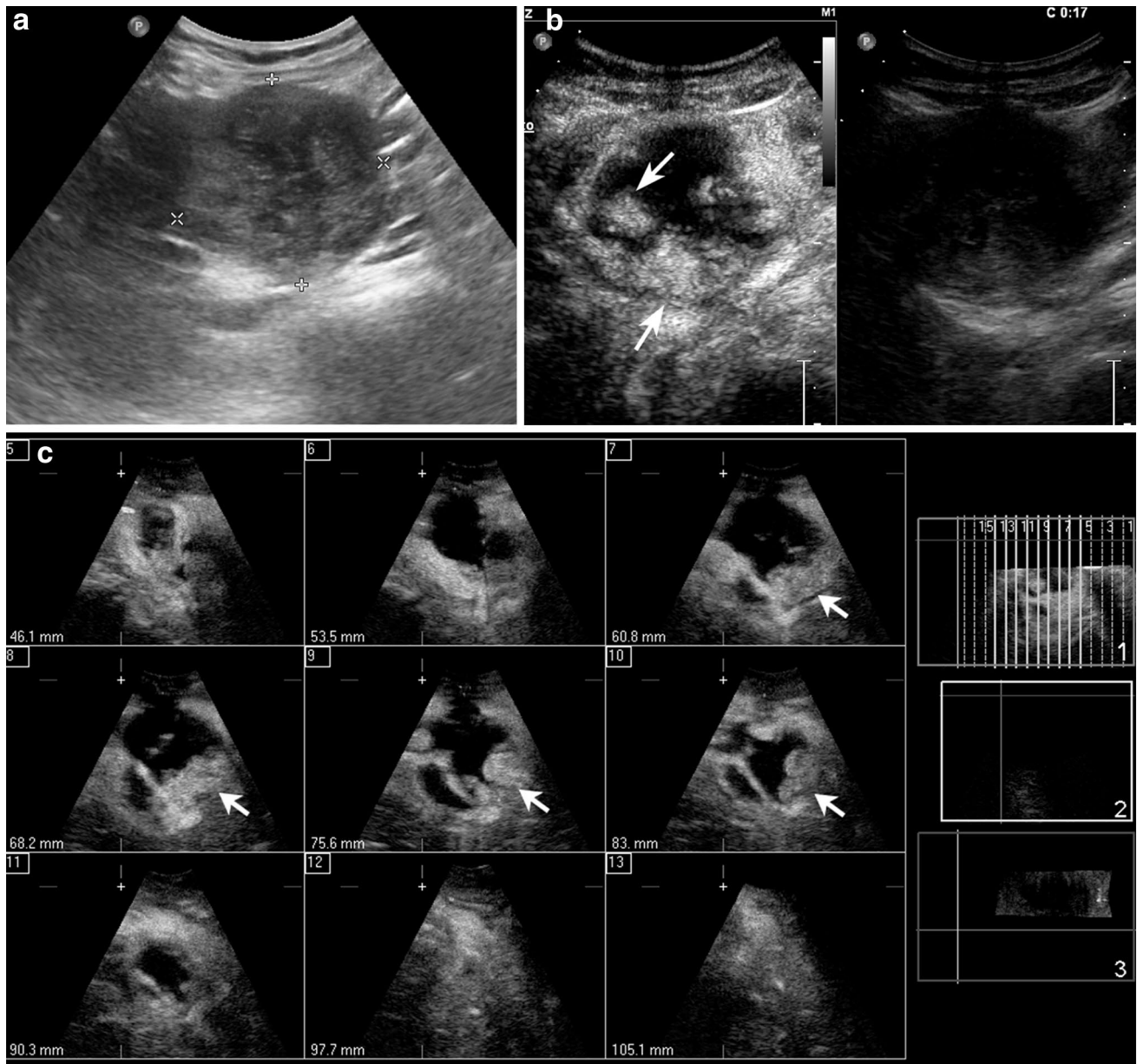


Fig. 3 Residual tumor after TACE. **a** Axial baseline image of the left lobe in a 52-year-old woman shows a 6.7 cm highly inhomogeneous mass (*calipers*); **b** 2D CEUS in the arterial phase (17 s after SonoVue

injection) shows a clear-cut hypervascularity within the treated area (*arrows*); **c** 3D i-Slice reconstruction (slice thickness 7.4 mm) depicts the same finding slice by slice (*arrows*)

adequate ablation of 97, 100, and 97 %, respectively [16]. Our experience, although in a more limited series and using mainly MRI as SOR, supports these observations and extends them to other modalities of locoregional treatment, such as TACE, PEI, and HABIB, with corresponding values of 91.7, 90.9, and 91.3 % respectively. In our series, we did not encounter a clinically relevant limitation of spatial resolution of the mechanical 3D probe regarding the non-linear imaging modes used in contrast-enhanced 3D studies as described by Leen and co-workers [8]. Besides the intervening technological improvement, an explanation for

this finding may be also found: (1) in the amount of contrast agent administered in our study: a full bolus of 4.8 mL of sulfur hexafluoride instead of the usually administered 2.4 mL dose, which allowed a better sensitivity of the technique to small vessels; (2) in the capability of displaying the region of interest as individual slices with a gap as thin as 0.1 mm, thus allowing the radiologist to better assess the presence of tiny foci of neovascularisation.

These latter observations may also explain the similar diagnostic performance of 3D CEUS to that of 2D CEUS observed in our series with excellent intermodality

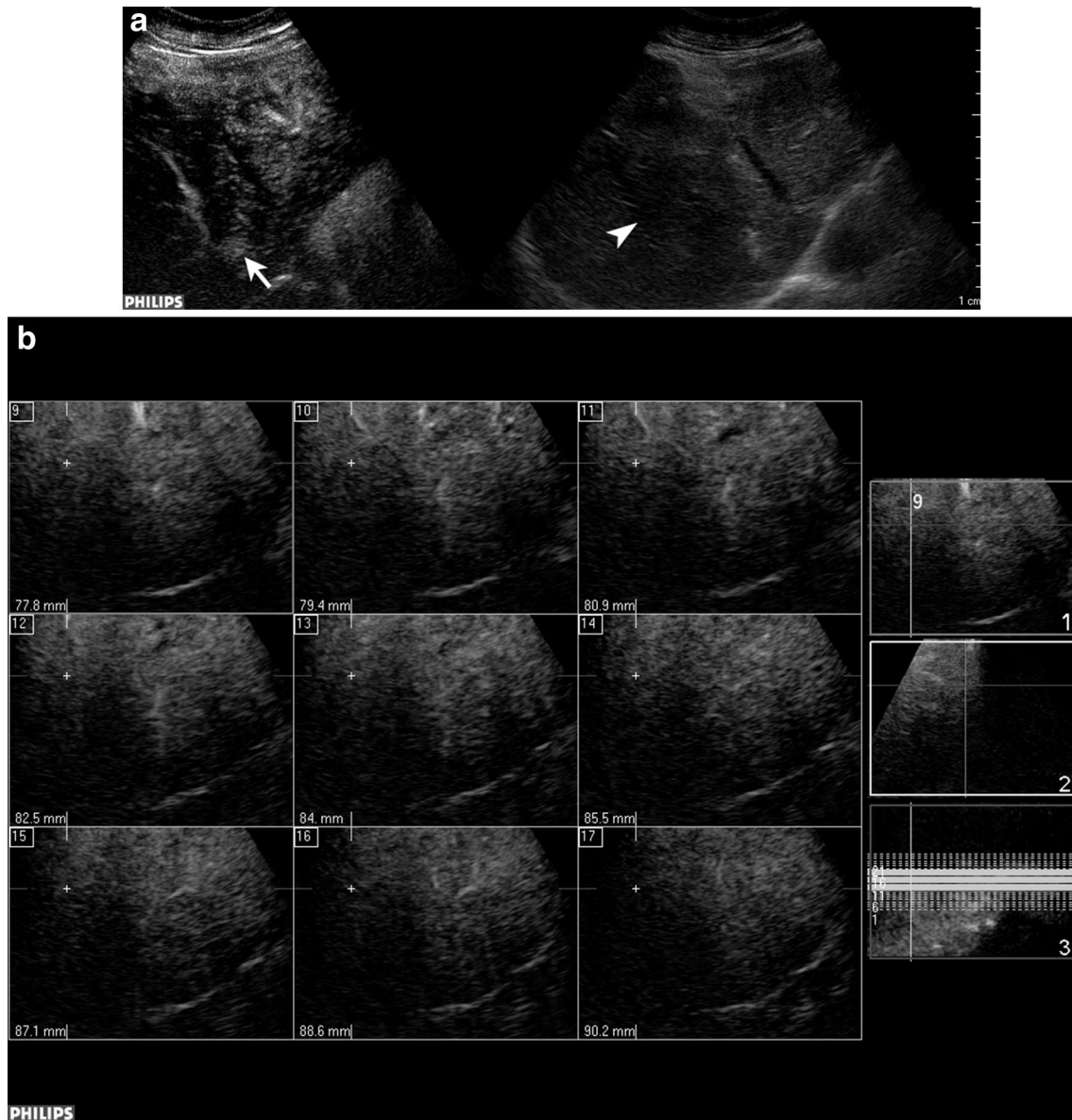


Fig. 4 False negative at 3D CEUS. **a** Oblique ascending right subcostal baseline US image in a 45-year-old woman with HCC treated by RFTA shows a barely visible area in the VIII hepatic segment (right, arrowhead). At 2D CEUS in the arterial phase, the lesion

shows a deeply located hypervascular focus at the periphery of the treated area suggestive of viable tumoral tissue (left, arrow); **b** residual tumor is not appreciable in any slice of 3D i-Slice reconstruction (slice thickness 1.5 mm)

agreement, thus encouraging a more extensive use of 3D CEUS in order to exploit the volumetric acquisition for a better assessment of tumoral geometry and orientation.

Nevertheless, in our series, such an improvement of sensitivity did not allow 3D CEUS to detect a residual tumor after RFA of a deeply located (100 mm) HCC sized 2 cm. This focus of still viable tumoral tissue was detected by 2D CEUS, probably because of its intrinsic capability of real-time evaluation of tumoral vascularisation. To this regard, 3D CEUS is more similar to MRI and CT, and further studies are needed to evaluate the improvement in spatial and

temporal resolution provided by the recently introduced new electronic matrix probes. Despite lacking real-time features, 3D CEUS appears to be promising in the calculation of tumor volume, definition of spatial geometry, and in detecting new foci of HCC occurring in patients already treated by means of LRT [8, 17, 18].

In our series, both 2D and 3D CEUS misdiagnosed a successfully RFA-treated HCC as residual tumor because of the presence of a peripherally located centimetric hypervascular nodule. At a retrospective analysis, this nodule did not show any appreciable washout. A four-year long

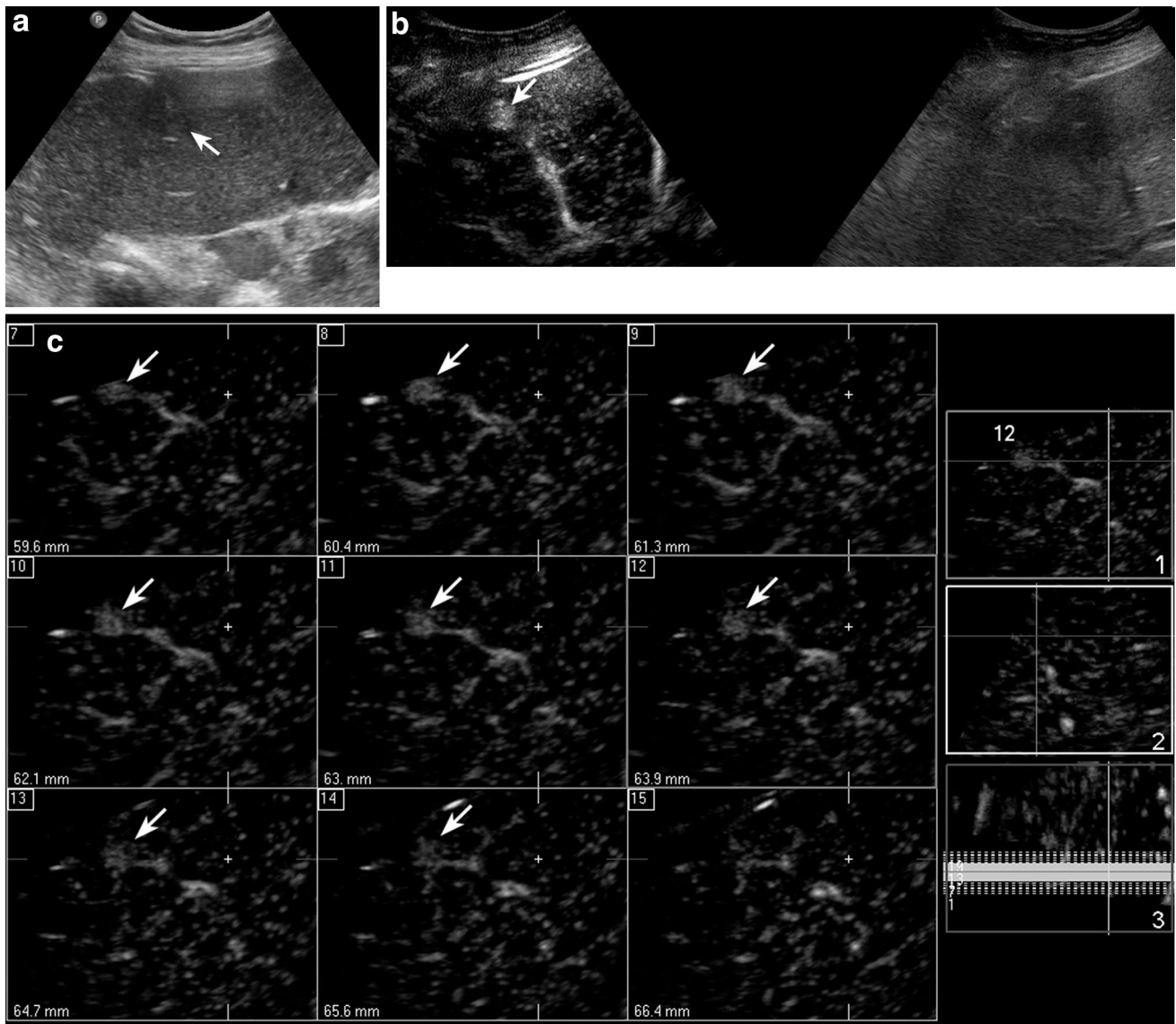


Fig. 5 False positive at 2D and 3D CEUS after PEI. **a** Axial baseline image of the right lobe in a 80-year-old woman shows a 3-cm subcapsular hypochoic area in the segment V (*arrow*). **b** 2D CEUS in the

arterial phase shows a hypervascular focus (*arrow*) at the periphery of the treated area; **c** 3D i-Slice reconstruction (slice thickness 0.9 mm) confirms the same finding slice by slice

follow-up with MR and CT confirmed the stability of this area, eventually considered as an arterial-dependent hyperperfusion defect following RFA which showed increased arterial contrast enhancement on all imaging modalities, including CT, MRI, and CEUS [19]. Although some authors consider any nodular arterially enhancing area within or along the margin of the ablated zone suspicious of viable tumor, our finding suggests that including the washout sign may improve the specificity in the detection of viable tumoral tissue after LRT [10, 20]. The presence of a thin peripheral rim of benign reactive hyperemia was observed in 2 cases, without misinterpretation by the readers. The rim of hyperemia may sometimes be difficult to

differentiate from actual residual tumor, but usually it should be thin, regular, completely surrounding the ablation area, and disappearing over time [6].

Time consumption does not seem to represent a major limitation of 3D CEUS technique, considering that in our experience a complete evaluation of each volumetric dataset lasted on average less than a minute.

This prospective study had some limitations. First, the patient population was relatively small. Second, we were not able to perform a pre-treatment 2D CEUS or 3D CEUS scan in order to compare them to post-treatment examination. This is the reason why we have only relied on vascularisation criteria of response to ablation and we have not

performed a volumetric assessment of treated area. Nevertheless, this limitation affects similarly either 2D CEUS or 3D CEUS. The third limitation was the lack of multiobserver evaluation for imaging analysis. Further studies are needed to address this specific issue.

In conclusion, in our preliminary experience, 2D and 3D CEUS provided similar diagnostic performance in the assessment of therapeutic response of HCC treated with LRT.

Conflict of interest The authors declare no conflict of interest.

Ethical standards This article does not contain any studies with human participants or animals performed by any of the authors.

References

- Dodd GD 3rd, Soulen MC, Kane RA et al (2000) Minimally invasive treatment of malignant hepatic tumors: at the threshold of a major breakthrough. *Radiographics* 20:9–27
- Taibbi A, Furlan A, Sandonato L et al (2012) Imaging findings of liver resection using a bipolar radiofrequency electrosurgical device-initial observations. *Eur J Radiol* 81:663–670
- Raza A, Sood GK (2014) Hepatocellular carcinoma review: current treatment, and evidence-based medicine. *World J Gastroenterol* 20:4115–4127
- Sala M, Llovet JM, Vilana R et al (2004) Initial response to percutaneous ablation predicts survival in patients with hepatocellular carcinoma. *Hepatology* 40:1352–1360
- El-Gazzaz G, Sourianarayanan A, Menon KV et al (2013) Radiologic-histological correlation of hepatocellular carcinoma treated via pre-liver transplant locoregional therapies. *Hepatobiliary Pancreat Dis Int* 12:34–41
- Bartolotta TV, Taibbi A, Midiri M, De Maria M (2008) Hepatocellular cancer response to radiofrequency tumor ablation: contrast-enhanced ultrasound. *Abdom Imaging* 33:501–511
- Luo W, Numata K, Morimoto M et al (2010) Role of Sonazoid-enhanced three-dimensional ultrasonography in the evaluation of percutaneous radiofrequency ablation of hepatocellular carcinoma. *Eur J Radiol* 75:91–97
- Leen E, Kumar S, Khan SA et al (2009) Contrast-enhanced 3D ultrasound in the radiofrequency ablation of liver tumors. *World J Gastroenterol* 15:289–299
- World Medical Association Declaration of Helsinki. Ethical principles for medical research involving human subjects. <http://www.wma.net/en/30publications/10policies/b3/>. Accessed 10 Oct 2014
- Yaghmai V, Besa C, Kim E et al (2013) Imaging assessment of hepatocellular carcinoma response to locoregional and systemic therapy. *AJR* 201:80–96
- Catalano O, Lobianco R, Esposito M et al (2001) Hepatocellular carcinoma recurrence after percutaneous ablation therapy: helical CT patterns. *Abdom Imaging* 26:375–383
- Limanond P, Zimmerman P, Raman SS et al (2003) Interpretation of CT and MRI after radiofrequency ablation of hepatic malignancies. *AJR* 181:1635–1640
- Xu HX, Lu MD, Xie XH et al (2009) Three-dimensional contrast-enhanced ultrasound of the liver: experience of 92 cases. *Ultrasonics* 49:377–385
- Luo W, Numata K, Morimoto M et al (2009) Three-dimensional contrast-enhanced sonography of vascular patterns of focal liver tumors: pilot study of visualization methods. *AJR* 192:165–173
- Luo W, Numata K, Morimoto M et al (2009) Focal liver tumors: characterization with 3D perflubutane microbubble contrast agent-enhanced US versus 3D contrast-enhanced multidetector CT. *Radiology* 251:287–295
- Luo W, Numata K, Morimoto M et al (2010) Role of Sonazoid-enhanced three-dimensional ultrasonography in the evaluation of percutaneous radiofrequency ablation of hepatocellular carcinoma. *Eur J Radiol* 75:91–97
- Bartolotta TV, Taibbi A, Matranga D et al (2012) Incidence of new foci of hepatocellular carcinoma after radiofrequency ablation: role of multidetector CT. *Radiol Med* 117:739–748
- Giangregorio F, Comparato G, Marinone MG et al (2009) Imaging detection of new HCCs in cirrhotic patients treated with different techniques: comparison of conventional US, spiral CT, and 3-dimensional contrast-enhanced US with the Navigator technique (Nav 3D CEUS). *J Ultrasound* 12:12–21
- Catalano O, Sandomenico F, Nunziata A et al (2007) Transient hepatic echogenicity difference on contrast-enhanced ultrasonography: sonographic sign and pitfall. *J Ultrasound Med* 26:337–345
- Zheng S-G, Xu H-X, Liu L-N et al (2014) Management of hepatocellular carcinoma: the role of contrast-enhanced ultrasound. *World J Radiol* 6:7–14